

Robust Tracking Control with Neural Network Dynamic Models under Input Perturbations

Huixuan Cheng^{1*} Hanjiang Hu^{1*} Changliu Liu¹

Abstract—Robust control problem has significant practical implication since external disturbances can significantly impact the performance of control method. Existing robust control method excels at control-affine system but fails at neural network dynamic models. Developing robust control methods for such systems remains a complex challenge. In this paper, we focus on robust tracking method for neural network dynamic models. We first propose reachability analysis tool designed for this system and then introduce how to reformulate robust tracking problem with the reachable sets. In addition, we prove the existence of feedback policy that bounds the growth of reachable set over infinite horizon. The effectiveness of proposed approach is validated through numerical tracking task simulations, where we compare it with a standard tube MPC method.

I. INTRODUCTION

Neural Network Dynamic Models (NNDMs) have emerged as a powerful alternative for modeling complex systems, leveraging the universal approximation theorem to capture system dynamics through a data-driven approach [1], [2]. This method simplifies model construction, particularly for systems where deriving accurate analytical models is challenging, time-intensive, or infeasible [3]. While NNDMs have been successfully applied to various control tasks [4], [5], ensuring robust tracking under perturbations in NNDM systems remains an underexplored yet crucial area. Given the prevalence of uncertainties and disturbances in real-world applications, robust tracking in NNDM systems is both practically important and technically challenging.

Existing robust control methods, such as robust Model Predictive Control (MPC), are well-established for control-affine systems [6], [7], [8]. However, these methods are inadequate for addressing the robust tracking problem in NNDMs due to the inherent nonlinearity, limited mathematical interpretability, and black-box nature of NNDMs. Traditional MPC methods, including tube-based MPC [9], [10] and its variations [11], [12], are not directly applicable to NNDMs due to these complexities. Other approaches like scenario-tree based MPC [13], [14] and system level parameterization [15] face scalability issues or are restricted to linear systems.

Our major insight to the robust tracking problem is that we could leverage neural network reachability analysis tools as a function of the control input to analyze the potential tracking error. By analyzing these reachable sets, we can

directly minimize tracking errors through the optimization of control sequences. This approach draws inspiration from recent advancements in computing approximate reachable sets for polynomial systems under time-varying uncertainties [16], [17]. While similar methods have been applied to polynomial-nonlinear robust MPC, our approach extends this concept to the more complex domain of NNDMs, addressing the unique challenges posed by neural network dynamics. Our contributions can be summarized as follows:

- We formulate a novel multi-step reachability analysis tool designed for NNDMs.
- We propose a robust tracking control method consisting of the reformulation of optimization problem based on reachability analysis and online optimization of control inputs.
- We conduct numerical experiments that demonstrate the efficacy of our method in terms of less control conservativeness and tracking error.

Notations: Minkowski sum of two sets \mathbb{A} and \mathbb{B} is given by $\mathbb{A} \oplus \mathbb{B} = \{\mathbf{a} + \mathbf{b} | \mathbf{a} \in \mathbb{A}, \mathbf{b} \in \mathbb{B}\}$. The Pontryagin difference between two sets \mathbb{A} and \mathbb{B} is given by $\mathbb{A} \ominus \mathbb{B} = \{\mathbf{a} | \mathbf{a} \oplus \mathbb{B} \subseteq \mathbb{A}\}$. The linear mapping between a matrix \mathbf{M} and a set \mathbb{A} is given by $\mathbf{M}\mathbb{A} = \{\mathbf{b} | \mathbf{b} = \mathbf{M}\mathbf{a}, \mathbf{a} \in \mathbb{A}\}$.

II. PROBLEM FORMULATION AND PRELIMINARY

A. Problem Formulation for NNDM

In this work, we consider the discrete-time Neural Network Dynamic Models (NNDM) with bounded perturbations on control inputs defined as follows

$$\mathbf{x}_{k+1} = \mathbf{x}_k + \mathbf{f}(\mathbf{x}_k, \mathbf{u}_k + \mathbf{w}_k)dt, \quad (1)$$

where dt is the sampling time interval, \mathbf{f} is the dynamic model parameterized by a deep neural network, $\mathbf{x}_k \in \mathbb{R}^{m_x}$ and $\mathbf{u}_k \in \mathbb{R}^{m_u}$ are state and control input at time k , and $\mathbf{w}_k \in \mathbb{R}^{m_u}$ is the bounded perturbation applied on \mathbf{u}_k at time k .

Assumption 1. The system dynamic $\mathbf{f} : \mathbb{R}^{m_x} \times \mathbb{R}^{m_u} \mapsto \mathbb{R}^{m_x}$ is assumed to be a n -layer feedforward neural networks with nonlinear activation functions. Specifically, $\mathbf{f} = \mathbf{f}_n \circ \mathbf{f}_{n-1} \circ \dots \circ \mathbf{f}_1$, where $\mathbf{f}_i : \mathbb{R}^{k_{i-1}} \mapsto \mathbb{R}^{k_i}$ is the i th linear mapping layer with a nonlinear activation $\sigma_i : \mathbb{R}^{k_i} \mapsto \mathbb{R}^{k_i}$ over the k_i -dimensional hidden variable in layer i .

We denote the weight matrix and bias vector in layer i as $\mathbf{W}_i \in \mathbb{R}^{k_i \times k_{i-1}}$ and $\mathbf{b}_i \in \mathbb{R}^{k_i}$, the hidden variable after the layer i is $\mathbf{z}_i = \mathbf{f}_i(\mathbf{z}_{i-1}) = \sigma_i(\hat{\mathbf{z}}_i)$, where $\hat{\mathbf{z}}_i = \mathbf{W}_i \mathbf{z}_{i-1} + \mathbf{b}_i$ is the pre-activation variable. For the input and output layers,

*The first two authors contributed equally.

¹Huixuan Cheng, Hanjiang Hu and Changliu Liu are with the Robotics Institute, Carnegie Mellon University, Pittsburgh, PA, 15213, USA. {huixuanc, hanjiangh, cliu6}@andrew.cmu.edu

it trivially holds that $\mathbf{z}_0 = [\mathbf{x}_k^\top, \mathbf{u}_k^\top]^\top$, $k_0 = m_x + m_u$, $k_n = m_x$. Let $W_{ij} \in \mathbb{R}^{1 \times k_{i-1}}$ be the j th row of \mathbf{W}_i and b_{ij} be the j th entry of \mathbf{b}_i , so the j th entry of $\hat{\mathbf{z}}_i$ is calculated as $\hat{z}_{ij} = W_{ij}z_{i-1} + b_{i,j}$. We only focus on ReLU activation in this work, so for the j th entry of \mathbf{z}_i , we have that $z_{ij} = \sigma_i(\hat{z}_{ij}) = \max\{0, \hat{z}_{ij}\}$.

Assumption 2. *The perturbation at each time k is within ℓ_∞ ball: $\|\mathbf{w}_k\|_\infty \leq \varepsilon_k$, where ε_k is the ℓ_∞ perturbation bound. At each time step, the perturbations are randomly sampled within their bound $\mathbf{w}_k \in \mathbb{W}_k = \{\mathbf{w} \mid \|\mathbf{w}\|_\infty \leq \varepsilon_k\}$.*

System constraints for state and control input are formulated as polytopic set containing the origin in their interior

$$\mathbb{X} = \{\mathbf{x} \in \mathbb{R}^{m_x} \mid \mathbf{H}_x \mathbf{x} \leq \mathbf{h}_x\}, \mathbb{U} = \{\mathbf{u} \in \mathbb{R}^{m_u} \mid \mathbf{H}_u \mathbf{u} \leq \mathbf{h}_u\} \quad (2)$$

The control problem is formulated as a N-step MPC tracking problem with quadratic costs and linear constraints.

Problem II.1.

$$\begin{aligned} \min \sum_{i=0}^{N-1} & ((\mathbf{x}_i - \mathbf{r}_i)^\top \mathbf{Q}(\mathbf{x}_i - \mathbf{r}_i) + \mathbf{u}_i^\top \mathbf{R} \mathbf{u}_i) \\ & + (\mathbf{x}_N - \mathbf{r}_N)^\top \mathbf{Q}_f(\mathbf{x}_N - \mathbf{r}_N) \\ \text{s.t. } & \mathbf{x}_{i+1} = \mathbf{x}_i + \mathbf{f}(\mathbf{x}_i, \mathbf{u}_i + \mathbf{w}_i) dt, \\ & \mathbf{x}_i \in \mathbb{X}, \mathbf{x}_N \in \mathbb{X}_f, \mathbf{u}_i + \mathbf{w}_i \in \mathbb{U}, \mathbf{w}_i \in \mathbb{W}_i \\ & i = 0, 1, \dots, N-1 \end{aligned} \quad (3)$$

where \mathbf{Q} , \mathbf{R} are positive semi-definite cost matrix, \mathbf{Q}_f is terminal cost matrix, N is control horizon, \mathbf{u}_i is control variable, \mathbf{r}_i is reference state, \mathbb{X} and \mathbb{U} are the state and action constraint defined in Equation (2), \mathbf{w}_i and \mathbb{W}_i are sampled perturbation and bounded perturbation set respectively.

B. Preliminaries

1) *Tube MPC:* The Tube MPC methods described in [9] address robust control problems for nonlinear systems by performing local linearization using Taylor series expansion at every time step. The linearized system $(\mathbf{A}_k, \mathbf{B}_k)$ at time k is as follows

$$\mathbf{x}_{k+1} = \mathbf{A}_k \mathbf{x}_k + \mathbf{B}_k \mathbf{u}_k + \mathbf{B}_k \mathbf{w}_k \quad (4)$$

$$\mathbf{A}_k = \frac{\partial \mathbf{f}}{\partial \mathbf{x}_k} dt + \mathbf{I}, \mathbf{B}_k = \frac{\partial \mathbf{f}}{\partial \mathbf{u}_k} dt \quad (5)$$

An important feature of tube MPC is that it splits dynamics with perturbations into a nominal system and a state error system and leverages feedback control method to bound state error as follows

$$\text{Nominal system } \hat{\mathbf{x}}_{k+1} = \mathbf{A}_k \hat{\mathbf{x}}_k + \mathbf{B}_k \hat{\mathbf{u}}_k \quad (6)$$

$$\text{State error system } \mathbf{e}_{k+1} = (\mathbf{A}_k + \mathbf{B}_k \mathbf{K}_k) \mathbf{e}_k + \mathbf{B}_k \mathbf{w}_k \quad (7)$$

$$\text{Feedback control } \mathbf{u}_k = \hat{\mathbf{u}}_k + \mathbf{K}_k (\mathbf{x}_k - \hat{\mathbf{x}}_k) \quad (8)$$

where $\hat{\mathbf{x}}_k, \hat{\mathbf{u}}_k$ are nominal state and control input without perturbations, $\mathbf{e}_k = \mathbf{x}_k - \hat{\mathbf{x}}_k$ is defined as state error. The feedback gain \mathbf{K}_k is chosen to make the state error system asymptotically stable and \mathbf{K}_k is only dependent on $\mathbf{A}_k, \mathbf{B}_k$.

Definition II.1. Disturbance invariant set \mathbb{Z}_k for linearized system $(\mathbf{A}_k, \mathbf{B}_k)$ at time k , as described in [18], satisfies

$$\text{for } \forall \mathbf{e}_i \in \mathbb{Z}_k, \forall \mathbf{w}_i \in \mathbb{W}_i, i = 0, 1, \dots \quad (9)$$

$$\mathbf{e}_{i+1} = (\mathbf{A}_k + \mathbf{B}_k \mathbf{K}_k) \mathbf{e}_i + \mathbf{B}_k \mathbf{w}_i \in \mathbb{Z}_k \quad (10)$$

where feedback control $\mathbf{u}_i = \hat{\mathbf{u}}_i + \mathbf{K}_k (\mathbf{x}_i - \hat{\mathbf{x}}_i)$ is applied. This set guarantees that for a fixed system $(\mathbf{A}_k, \mathbf{B}_k)$, even under the influence of bounded disturbances, the error of system states will not leave this set over time.

Definition II.2. Nominal optimization problem is solving the tracking problem with nominal system as dynamic constraints. Nominal optimization problem can be formulated as:

$$\begin{aligned} \min \sum_{i=0}^{N-1} & ((\hat{\mathbf{x}}_i - \mathbf{r}_i)^\top \mathbf{Q}(\hat{\mathbf{x}}_i - \mathbf{r}_i) + \hat{\mathbf{u}}_i^\top \mathbf{R} \hat{\mathbf{u}}_i) \\ & + (\hat{\mathbf{x}}_N - \mathbf{r}_N)^\top \mathbf{Q}_f(\hat{\mathbf{x}}_N - \mathbf{r}_N) \\ \text{s.t. } & \hat{\mathbf{x}}_{i+1} = \hat{\mathbf{x}}_i + \mathbf{f}(\hat{\mathbf{x}}_i, \hat{\mathbf{u}}_i) dt, \\ & \hat{\mathbf{x}}_i \in \mathbb{X}, \hat{\mathbf{x}}_N \in \mathbb{X}_f, \hat{\mathbf{u}}_i \in \mathbb{U} \\ & i = 0, 1, \dots, N-1 \end{aligned} \quad (11)$$

The disturbance invariant set for the linearized system at time k , denoted as \mathbb{Z}_k , can be computed as an infinite Minkowski sum: $\mathbb{Z}_k = \mathbf{B}_k \mathbb{W}_k \oplus (\mathbf{A}_k + \mathbf{B}_k \mathbf{K}_k) \mathbf{B}_k \mathbb{W}_k \oplus (\mathbf{A}_k + \mathbf{B}_k \mathbf{K}_k)^2 \mathbf{B}_k \mathbb{W}_k \oplus \dots$. Robustness of tracking problem can be guaranteed by incorporating \mathbb{Z}_k into constraints of nominal optimization problem and apply feedback control according to nominal solutions. The nominal tracking problem at time step k can then be reformulated as follows

$$\begin{aligned} \min \sum_{i=0}^{N-1} & ((\hat{\mathbf{x}}_i - \mathbf{r}_i)^\top \mathbf{Q}(\hat{\mathbf{x}}_i - \mathbf{r}_i) + \hat{\mathbf{u}}_i^\top \mathbf{R} \hat{\mathbf{u}}_i) \\ & + (\hat{\mathbf{x}}_N - \mathbf{r}_N)^\top \mathbf{Q}_f(\hat{\mathbf{x}}_N - \mathbf{r}_N) \\ \text{s.t. } & \hat{\mathbf{x}}_{i+1} = \hat{\mathbf{x}}_i + \mathbf{f}(\hat{\mathbf{x}}_i, \hat{\mathbf{u}}_i) dt, \\ & \hat{\mathbf{x}}_i \in \mathbb{X} \ominus \mathbb{Z}_k, \hat{\mathbf{x}}_N \in \mathbb{X}_f \ominus \mathbb{Z}_k, \\ & \hat{\mathbf{u}}_i \in \mathbb{U} \ominus \mathbf{K}_k \mathbb{Z}_k \ominus \mathbb{W}_i, i = 0, 1, \dots, N-1 \end{aligned} \quad (12)$$

After solving nominal optimization problem and obtain solutions $\hat{\mathbf{u}}_0, \dots, \hat{\mathbf{u}}_{N-1}$, we apply feedback control as $\mathbf{u}_k = \hat{\mathbf{u}}_k + \mathbf{K}_k (\mathbf{x}_k - \hat{\mathbf{x}}_k)$ which guarantees constraint satisfaction in Problem II.1 during control process with disturbance.

2) *Reachability for Neural Networks:* Reachability analysis for NNDMs has been widely used in neural network verification [19], which provides symbolic linear bound for neural network output given perturbed input within a specific range.

Definition II.3. Symbolic linear bound For a neural network with input data $[\mathbf{x}_{k-1}^\top, \mathbf{u}_{k-1}^\top]^\top$ perturbed within a ϵ -bounded l_p -ball, the symbolic linear bound is computed as:

$$\underline{\mathbf{W}}_{\mathbf{x}_k}^x \begin{bmatrix} \mathbf{x}_{k-1} \\ \mathbf{u}_{k-1} \end{bmatrix} + \underline{\mathbf{b}}_{\mathbf{x}_k}^x \leq \mathbf{x}_k \leq \overline{\mathbf{W}}_{\mathbf{x}_k}^x \begin{bmatrix} \mathbf{x}_{k-1} \\ \mathbf{u}_{k-1} \end{bmatrix} + \overline{\mathbf{b}}_{\mathbf{x}_k}^x \quad (13)$$

where $\underline{\mathbf{W}}_{\mathbf{x}_k}^x, \overline{\mathbf{W}}_{\mathbf{x}_k}^x \in \mathbb{R}^{m_x \times (m_x + m_u)}$, $\underline{\mathbf{b}}_{\mathbf{x}_k}^x, \overline{\mathbf{b}}_{\mathbf{x}_k}^x \in \mathbb{R}^{m_x}$ are weights and biases dependent on $[\mathbf{x}_{k-1}^\top, \mathbf{u}_{k-1}^\top]^\top$ and ϵ . And

$\mathbf{x}_{k-1}, \mathbf{u}_{k-1}$ are symbolic variables which can be selected their exact value within perturbation bound while guarantees the soundness of linear bound.

The symbolic linear bounds are primarily derived using interval arithmetic at the hidden layers and linear relaxations at ReLU-activated layers, as outlined in [20]. The calculation of $\underline{\mathbf{W}}_{x_k}^x, \overline{\mathbf{W}}_{x_k}^x, \underline{\mathbf{b}}_{x_k}^x, \overline{\mathbf{b}}_{x_k}^x$ is propagated from the input layer to the output layer, based on the weights, biases from the hidden layers, and the selection of linear relaxation bounds for the ReLU units.

3) *Challenges*: Based on the information above, the challenges of solving robust tracking problem with perturbations on control input can be summarized as follows

- The tube MPC method introduces errors into the disturbance invariant set due to linearizing nonlinear dynamics, often resulting in an overly conservative disturbance invariant set as described in [21]
- Verification methods typically provide bounds for neural networks rather than directly addressing NNDMs, making it non-trivial to obtain tight reachability analysis for NNDMs over the look-ahead horizon.

III. REACHABILITY-BASED ROBUST MPC FOR NNDMS

In this section, we first present how to develop multi-step reachability analysis for NNDMs without linearization of system dynamic. Next, we introduce the reformulation of the robust tracking problem given the reachable set. Last, we show the procedure for online execution and how the optimization problem is solved online.

A. Reachability analysis and robust tracking problem

We present a k -step reachability analysis tool for NNDMs based on the verification method outlined in Section II-B.2, bridging the gap between neural network verification and reachability computation for NNDMs.

Definition III.1. Operation of $(\cdot)_+$ is defined as $(\cdot)_+ = \text{ReLU}(\cdot)$ and $(\cdot)_-$ is defined as $(\cdot)_- = -\text{ReLU}(-\cdot)$, where $\text{ReLU}(\cdot)$ means applying ReLU operation element-wise.

Theorem III.1. For a NNDM system satisfying Equation (1), k is any time step, reachable set of \mathbf{x}_k can be bounded linearly by $\mathbf{x}_0, \mathbf{u}_0, \dots, \mathbf{u}_{k-2}, \mathbf{u}_{k-1}$ variables. Weights and biases of linear bound w.r.t. these variables can be obtained recursively as follows:

$$\underline{\mathbf{W}}_k^x \begin{bmatrix} \mathbf{x}_0 \\ \mathbf{u}_0 \\ \dots \\ \mathbf{u}_{k-1} \end{bmatrix} + \underline{\mathbf{b}}_k^x \leq \mathbf{x}_k \leq \overline{\mathbf{W}}_k^x \begin{bmatrix} \mathbf{x}_0 \\ \mathbf{u}_0 \\ \dots \\ \mathbf{u}_{k-1} \end{bmatrix} + \overline{\mathbf{b}}_k^x \quad (14)$$

where $\underline{\mathbf{W}}_1^x = \underline{\mathbf{W}}_{x_k}^x, \overline{\mathbf{W}}_1^x = \overline{\mathbf{W}}_{x_k}^x; \underline{\mathbf{b}}_1^x = \underline{\mathbf{b}}_{x_k}^x, \overline{\mathbf{b}}_1^x = \overline{\mathbf{b}}_{x_k}^x$

$$\begin{cases} \underline{\mathbf{W}}_{i+1}^x = (\underline{\mathbf{W}}_i^x)_+ \begin{bmatrix} \underline{\mathbf{W}}_{x_{k-i}}^x & \mathbf{0} \\ \mathbf{0} & \mathbf{I}_{i \cdot m_u} \end{bmatrix} + (\underline{\mathbf{W}}_i^x)_- \begin{bmatrix} \overline{\mathbf{W}}_{x_{k-i}}^x & \mathbf{0} \\ \mathbf{0} & \mathbf{I}_{i \cdot m_u} \end{bmatrix} \\ \overline{\mathbf{W}}_{i+1}^x = (\overline{\mathbf{W}}_i^x)_+ \begin{bmatrix} \overline{\mathbf{W}}_{x_{k-i}}^x & \mathbf{0} \\ \mathbf{0} & \mathbf{I}_{i \cdot m_u} \end{bmatrix} + (\overline{\mathbf{W}}_i^x)_- \begin{bmatrix} \underline{\mathbf{W}}_{x_{k-i}}^x & \mathbf{0} \\ \mathbf{0} & \mathbf{I}_{i \cdot m_u} \end{bmatrix} \\ \underline{\mathbf{b}}_{i+1}^x = \underline{\mathbf{b}}_i^x + (\underline{\mathbf{W}}_i^x)_+ \begin{bmatrix} \underline{\mathbf{b}}_{x_{k-i}}^x \\ \mathbf{0}_{i \cdot m_u} \end{bmatrix} + (\underline{\mathbf{W}}_i^x)_- \begin{bmatrix} \overline{\mathbf{b}}_{x_{k-i}}^x \\ \mathbf{0}_{i \cdot m_u} \end{bmatrix} \\ \overline{\mathbf{b}}_{i+1}^x = \overline{\mathbf{b}}_i^x + (\overline{\mathbf{W}}_i^x)_+ \begin{bmatrix} \overline{\mathbf{b}}_{x_{k-i}}^x \\ \mathbf{0}_{i \cdot m_u} \end{bmatrix} + (\overline{\mathbf{W}}_i^x)_- \begin{bmatrix} \underline{\mathbf{b}}_{x_{k-i}}^x \\ \mathbf{0}_{i \cdot m_u} \end{bmatrix} \end{cases}$$

$\underline{\mathbf{W}}_i^x, \overline{\mathbf{W}}_i^x \in \mathbb{R}^{m_x \times (m_x + i \cdot m_u)}, \underline{\mathbf{b}}_i^x, \overline{\mathbf{b}}_i^x \in \mathbb{R}^{m_x}, i = 1, 2, \dots, k-1,$

and $\overline{\mathbf{W}}_{x_{k-i}}^x, \underline{\mathbf{W}}_{x_{k-i}}^x, \underline{\mathbf{b}}_{x_{k-i}}^x, \overline{\mathbf{b}}_{x_{k-i}}^x$ represent the weights and biases for the symbolic linear bound of the state \mathbf{x}_{k-i} , derived using Section II-B.2. Similarly, $\underline{\mathbf{W}}_k^x, \underline{\mathbf{b}}_k^x, \overline{\mathbf{W}}_k^x, \overline{\mathbf{b}}_k^x$ are the weights and biases that construct the linear bound of the reachable set for \mathbf{x}_k , depending on the region of input sequence $(\mathbf{x}_0, \mathbf{u}_0, \dots, \mathbf{u}_{k-2}, \mathbf{u}_{k-1})$.

Proof. We prove this inequality by proving a stronger inequality as follow, where $l = 1, \dots, k$

$$\underline{\mathbf{W}}_l^x \begin{bmatrix} \mathbf{x}_{k-l} \\ \mathbf{u}_{k-l} \\ \dots \\ \mathbf{u}_{k-1} \end{bmatrix} + \underline{\mathbf{b}}_l^x \leq \mathbf{x}_k \leq \overline{\mathbf{W}}_l^x \begin{bmatrix} \mathbf{x}_{k-l} \\ \mathbf{u}_{k-l} \\ \dots \\ \mathbf{u}_{k-1} \end{bmatrix} + \overline{\mathbf{b}}_l^x \quad (15)$$

We use mathematical induction to prove Equation (15) holds for $l = 1, \dots, k$, with the case $l = k$ establishing Theorem III.1. First when $l = 1$, Equation (15) reduces to symbolic linear bound in Section II-B.2, which trivially holds. Assume Equation (15) holds for $l = n, (n < k-1)$, where the reachable set of \mathbf{x}_k can be linearly bounded by $\mathbf{x}_{k-n}, \mathbf{u}_{k-n}, \dots, \mathbf{u}_{k-1}$. We then substitute symbolic bound of \mathbf{x}_{k-n} into $l = n$ inequality and rearrange it as follows

$$\begin{aligned} & \left((\underline{\mathbf{W}}_n^x)_+ \begin{bmatrix} \underline{\mathbf{W}}_{x_{k-n}}^x & \mathbf{0} \\ \mathbf{0} & \mathbf{I}_{n \cdot m_u} \end{bmatrix} + (\underline{\mathbf{W}}_n^x)_- \begin{bmatrix} \overline{\mathbf{W}}_{x_{k-n}}^x & \mathbf{0} \\ \mathbf{0} & \mathbf{I}_{n \cdot m_u} \end{bmatrix} \right) \begin{bmatrix} \mathbf{x}_{k-n-1} \\ \mathbf{u}_{k-n-1} \\ \dots \\ \mathbf{u}_{k-1} \end{bmatrix} \\ & + \underline{\mathbf{b}}_n^x + (\underline{\mathbf{W}}_n^x)_+ \begin{bmatrix} \underline{\mathbf{b}}_{x_{k-n}}^x \\ \mathbf{0}_{n \cdot m_u} \end{bmatrix} + (\underline{\mathbf{W}}_n^x)_- \begin{bmatrix} \overline{\mathbf{b}}_{x_{k-n}}^x \\ \mathbf{0}_{n \cdot m_u} \end{bmatrix} \leq \mathbf{x}_k \leq \\ & \left((\overline{\mathbf{W}}_n^x)_+ \begin{bmatrix} \overline{\mathbf{W}}_{x_{k-n}}^x & \mathbf{0} \\ \mathbf{0} & \mathbf{I}_{n \cdot m_u} \end{bmatrix} + (\overline{\mathbf{W}}_n^x)_- \begin{bmatrix} \underline{\mathbf{W}}_{x_{k-n}}^x & \mathbf{0} \\ \mathbf{0} & \mathbf{I}_{n \cdot m_u} \end{bmatrix} \right) \begin{bmatrix} \mathbf{x}_{k-n-1} \\ \mathbf{u}_{k-n-1} \\ \dots \\ \mathbf{u}_{k-1} \end{bmatrix} \\ & + \overline{\mathbf{b}}_n^x + (\overline{\mathbf{W}}_n^x)_+ \begin{bmatrix} \overline{\mathbf{b}}_{x_{k-n}}^x \\ \mathbf{0}_{n \cdot m_u} \end{bmatrix} + (\overline{\mathbf{W}}_n^x)_- \begin{bmatrix} \underline{\mathbf{b}}_{x_{k-n}}^x \\ \mathbf{0}_{n \cdot m_u} \end{bmatrix} \end{aligned}$$

where the weight and bias align with iterations in Theorem III.1. Thus Equation (15) holds when $l = k$, thereby proving Theorem III.1. \square \square

Corollary III.2. Given the linear bound of the reachable set for \mathbf{x}_k in Theorem III.1 and lower and upper bounds of $\mathbf{u}_0, \dots, \mathbf{u}_{k-1}$, sound concrete reachable set for \mathbf{x}_k , denoted as \mathbb{R}_k can be derived by applying interval arithmetic in [20].

$$\mathbb{R}_k = \{ \mathbf{x} : \mathbf{x} \geq (\underline{\mathbf{W}}_k^x)_+ \begin{bmatrix} \underline{\mathbf{x}}_0 \\ \underline{\mathbf{u}}_0 \\ \dots \\ \underline{\mathbf{u}}_{k-1} \end{bmatrix} + (\underline{\mathbf{W}}_k^x)_- \begin{bmatrix} \overline{\mathbf{x}}_0 \\ \overline{\mathbf{u}}_0 \\ \dots \\ \overline{\mathbf{u}}_{k-1} \end{bmatrix} + \underline{\mathbf{b}}_k^x, \quad (16)$$

$$\mathbf{x} \leq (\overline{\mathbf{W}}_k^x)_- \begin{bmatrix} \underline{\mathbf{x}}_0 \\ \underline{\mathbf{u}}_0 \\ \dots \\ \underline{\mathbf{u}}_{k-1} \end{bmatrix} + (\overline{\mathbf{W}}_k^x)_+ \begin{bmatrix} \overline{\mathbf{x}}_0 \\ \overline{\mathbf{u}}_0 \\ \dots \\ \overline{\mathbf{u}}_{k-1} \end{bmatrix} + \overline{\mathbf{b}}_k^x, \mathbf{x} \in \mathbb{R}^{m_x} \} \quad (17)$$

where $\underline{\mathbf{W}}_k^x, \underline{\mathbf{b}}_k^x, \overline{\mathbf{W}}_k^x, \overline{\mathbf{b}}_k^x$ are weights and biases in Equation (15), $(\cdot), (\cdot)$ implies lower and upper bounds of the value and \geq, \leq represent element-wise comparison.

Here we need to emphasize that reachable set \mathbb{R}_k in Theorem III.2 is dependent on $\underline{x}_0, \bar{x}_0, \underline{u}_0, \bar{u}_0, \underline{u}_1, \bar{u}_1, \dots, \underline{u}_{k-1}, \bar{u}_{k-1}$, and \mathbb{R}_k can be referred as a function of these variables. The function can be defined as $\mathbb{R}_k = R_k^\varepsilon(\underline{x}_0, \underline{u}_0, \dots, \underline{u}_{k-1})$, where $\varepsilon = (\varepsilon_0, \varepsilon_1, \dots, \varepsilon_{k-1})$, and $\underline{x}_0 = \underline{x}_0, \bar{x}_0, \underline{u}_i = \underline{u}_i - \varepsilon_i, \bar{u}_i = \underline{u}_i + \varepsilon_i, i = 0, 1, \dots, k-1$. Reachable set \mathbb{R}_k encodes that all perturbed state is within this set, which means that $\underline{x}_k \in \mathbb{R}_k, \hat{x}_k \in \mathbb{R}_k$. For robustness control, \mathbb{R}_k should be within the state constraint $\mathbb{R}_k \subseteq \mathbb{X}$ to guarantee constraints satisfaction.

Based on the reachability analysis, we could ensure the robustness of the tracking problem by incorporating the sound reachable sets into problem constraints. The nominal tracking problem at time step k can be reformulated as follows

$$\begin{aligned} & \min \sum_{i=0}^{N-1} ((\hat{x}_i - r_i)^\top Q (\hat{x}_i - r_i) + \hat{u}_i^\top R \hat{u}_i) \\ & + (\hat{x}_N - r_N)^\top Q_f (\hat{x}_N - r_N) \\ \text{s.t. } & \hat{x}_{i+1} = \hat{x}_i + f(\hat{x}_i, \hat{u}_i) dt, \\ & \mathbb{R}_k^\varepsilon(\hat{x}_0, \hat{u}_0, \dots, \hat{u}_i) \subseteq \mathbb{X}, \mathbb{R}_N^\varepsilon(\hat{x}_0, \hat{u}_0, \dots, \hat{u}_N) \subseteq \mathbb{X}_f, \\ & \hat{u}_i \in \mathbb{U} \ominus \mathbb{W}_i, i = 0, 1, \dots, N-1 \end{aligned} \quad (18)$$

where \hat{x}_0 is a fixed and known variable and $\hat{u}_0, \hat{u}_1, \dots, \hat{u}_{N-1}$ are decision variables.

After solving nominal optimization problem and obtain solutions $\hat{u}_0, \dots, \hat{u}_{N-1}$, we apply control as $\underline{u}_k = \hat{u}_0$ which guarantees constraint satisfaction in Problem II.1 during control process with disturbance.

The key difference between the reachability-based formulation in Problem 18 and the tube MPC problem in Problem 12 lies in the treatment of state constraints. Tube MPC relies on a disturbance invariant set that is dependent on the linearized system dynamics matrices A_k and B_k , which can lead to inaccuracies and over-conservatism, as previously noted. In contrast, the reachability-based problem uses time-dependent reachable sets as state constraints, which are computed directly from the neural network dynamics rather than linearized models.

The relationship between disturbance invariant set \mathbb{Z}_k in Problem 12 and reachable set \mathbb{R}_i in Problem 18 is straightforward. Disturbance invariant set \mathbb{Z}_k bounds the state error $e_i = \underline{x}_i - \hat{x}_i$, whereas the reachable set \mathbb{R}_i bounds the perturbed state \underline{x}_i . When applying disturbance invariant set to the nominal state we obtain reachable set of state for tube MPC method denoted as $R_i^{tube} = \hat{x}_i \oplus \mathbb{Z}_k$. Comparing the conservativeness, i.e. the volume, of the disturbance invariant set in tube MPC and reachable set in our method is meaningful because both of them represent the distance from nominal state and measure the level of perturbation. However, the time-dependent nature of reachable set in our method provides much tighter bounds, effectively reducing conservativeness, as demonstrated empirically in Section IV. As a result, the challenges encountered in tube MPC can be addressed by employing the reachability-based method.

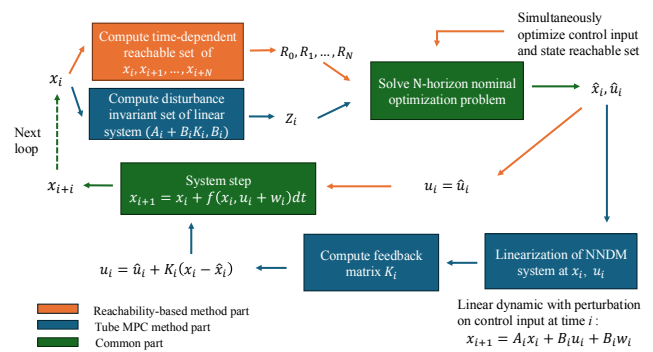


Fig. 1. Comparison between the proposed reachability-based method and the tube MPC method during online computation.

Remark. Given the information above, we could also control the growth of the reachable set through a feedback control as $\underline{u}_k = \hat{u}_k + G_k(\underline{x}_k - \hat{x}_k)$, where G_k is the feedback matrix at time k . Using reachability tool, we can derive symbolic bound for \underline{x}_{k+1} as demonstrated in Equation (13)

$$\underline{x}_{k+1} \leq \overline{W}_{x_{k+1}}^f \underline{x}_k + \overline{W}_{u_{k+1}}^f \underline{u}_k + \overline{b}_{x_{k+1}}^x \quad (19)$$

$$\underline{x}_{k+1} \geq \underline{W}_{x_{k+1}}^f \underline{x}_k + \underline{W}_{u_{k+1}}^f \underline{u}_k + \underline{b}_{x_{k+1}}^x \quad (20)$$

where $[\overline{W}_{x_{k+1}}^f; \overline{W}_{u_{k+1}}^f] = \overline{W}_{x_{k+1}}^x, [\underline{W}_{x_{k+1}}^f; \underline{W}_{u_{k+1}}^f] = \underline{W}_{x_{k+1}}^x$. We assume a simplified case where the difference of $\overline{W}_{x_{k+1}}^f - \underline{W}_{x_{k+1}}^f$ and $\overline{W}_{u_{k+1}}^f - \underline{W}_{u_{k+1}}^f$ are small and can be bounded by

$$\|\overline{W}_{x_{k+1}}^f - \underline{W}_{x_{k+1}}^f\|_\infty \leq \gamma \quad (21)$$

$$\|\overline{W}_{u_{k+1}}^f - \underline{W}_{u_{k+1}}^f\|_\infty \leq \gamma \quad (22)$$

Under this assumption, there exist a feedback matrix G_k that simultaneously stabilizes both $\overline{W}_{x_{k+1}}^f + \overline{W}_{u_{k+1}}^f G_k$ and $\underline{W}_{x_{k+1}}^f + \underline{W}_{u_{k+1}}^f G_k$, which further leads to bounded reachable sets as k increases over a long horizon. Simulation results in the DubinsCar environment, presented in Section IV-C.2, confirm the existence of such a feedback matrix. Future work may explore more general feedback policies to further bound the reachable sets and how to obtain forward invariant set in the presence of disturbances based on the bounded reachable sets.

B. Online control

The online execution procedure for the robust tracking problem entails solving a nonlinear optimization problem at each time step k . This optimization problem, formulated in Equation (18), aims to minimize a cost function by simultaneously optimizing control inputs and their associated reachable sets, subject to reformulated state constraints. These state constraints incorporate reachable sets to ensure robustness against disturbances. To efficiently solve this optimization problem, we employ a numerical optimization solver, specifically IPOPT (Interior Point OPTimizer), as detailed in [22].

The problem is inherently a Mixed Integer Programming (MIP) task. Although the NNNDM dynamics are nonlinear, they can be decomposed into several linear constraints and mixed-integer constraints. All hidden layers in \mathbf{f} are represented as linear constraints, and we introduce integers to encode the ReLU activation layer, as detailed in [5]. The implementation of an MIP solver is something we plan to explore in the future. The online execution procedure, which contrasts with the tube MPC approach, is illustrated in Figure 1.

IV. NUMERICAL STUDY

In this section, we aim to use numerical examples to show: the existence of feedback control to bound the reachable set over a long horizon, and a comparison between the tube MPC method and the reachability analysis method in terms of the conservativeness of the disturbance invariant set and control cost when solving robust tracking problems. We begin by outlining the problem settings in the Pendulum and DubinsCar environments within RobotZoo.jl, as illustrated in Figure 2, followed by an evaluation of the effectiveness of our approach.

A. Simulation set up

We utilize neural network-approximated dynamics for the Pendulum and DubinsCar environments, trained via a supervised learning approach with mean square error (MSE) as the loss function. The well-fitted neural networks are treated as the true dynamics in Equation (1), with a discrete time interval of $dt = 0.1$. Perturbations on the control input along the trajectory are randomly sampled within a constant l_∞ bound, implying that $\mathbb{W}_0 = \mathbb{W}_1 = \dots = \mathbb{W}_i = \dots = \mathbb{W} = \{\mathbf{w} \in \mathbb{R} \mid \|\mathbf{w}\|_\infty \leq \varepsilon\}$. For both scenarios, we consider a 1-step look-ahead robust tracking problem without loss of generality. Extending this to a multi-step look-ahead will be addressed in future work. These examples are implemented in Julia, and the nominal tracking problems are solved using IPOPT [22].

The comparison is made between our proposed method and the conventional tube MPC method, introduced in Section II-B.1 and Section III-B, respectively. In the following figures and tables, the label *Baseline* refers to the tube-based approach, while *Ours* denotes the reachability-based robust MPC for NNNDMs.

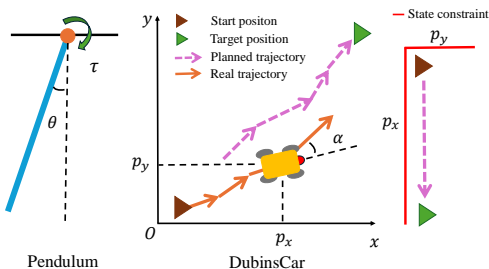


Fig. 2. Illustration of Pendulum and DubinsCar scenarios.

B. Robust tracking problem design

In the Pendulum environment, the state and action are $\mathbf{x} = [\theta, \dot{\theta}]^\top$, $\mathbf{u} = \tau$, where θ and $\dot{\theta}$ denote angle and angular velocity relative to the vertical direction, and τ the torque at the support point, as shown in Figure 2. The constraints are $\mathbb{X} = \{\mathbf{x} \in \mathbb{R}^2 \mid [-\pi, \pi] \times [-10, 10]\}$, $\mathbb{U} = \{u \in \mathbb{R} \mid |u| \leq 10\}$, $\mathbb{W} = \{\mathbf{w} \in \mathbb{R} \mid \|\mathbf{w}\|_\infty \leq \varepsilon\}$. State reference of the tracking task is a trajectory of constant angular velocity lifting from the equilibrium point, where $\theta_r = 0.12t$, $\dot{\theta}_r = 0.12$. Cost matrices are formulated as $\mathbf{Q} = \mathbf{I}_2$, $\mathbf{R} = 0.01$.

In DubinsCar, the state and action are $\mathbf{x} = [p_x, p_y, \alpha]^\top$, $\mathbf{u} = [v, \phi]$, where p_x, p_y are positions, α is the orientation angle, v, ϕ are velocity and angular velocity respectively, as shown in Figure 2. The constraints are $|p_x|, |p_y| \leq 1$, $|\alpha| \leq \pi$, $|v|, |\phi| \leq 5$ and $\mathbb{W} = \{\mathbf{w} \in \mathbb{R} \mid \|\mathbf{w}\|_\infty \leq \varepsilon\}$. In this scenario, we consider a planner to assist in the reference tracking process. State at time i is represented as $\mathbf{x}_i = [p_x^i, p_y^i, \alpha^i]^\top$. Target state $\mathbf{x}_r = [p_x^r, p_y^r, 0]^\top$ is a specific position with $\alpha = 0$. Planning state $\mathbf{x}_p^i = [p_{x,p}^i, p_{y,p}^i, \alpha_p^i]^\top$ is generated at each time step i according to current state \mathbf{x}_i , where $\alpha_p^i = \arctan\left(\frac{p_y^r - p_y^i}{p_x^r - p_x^i}\right)$, and $[p_{x,p}^i, p_{y,p}^i]^\top$ is a segment point on the line connecting $[p_x^i, p_y^i]^\top$ and $[p_x^r, p_y^r]^\top$, where the projection along the x and y directions does not exceed 0.08. Robust tracking problem treats \mathbf{x}_p^i as reference and cost matrices are $\mathbf{Q} = \mathbf{I}_3$, $\mathbf{R} = 0.01\mathbf{I}_2$.

C. Results and discussion

1) *Pendulum*: We randomly sample 50 initial states from the set $\{[\theta, \dot{\theta}]^\top \mid |\theta| \leq \pi/2, \dot{\theta} = 0\}$ and apply control for 50 steps for each instance. The left figure of Figure 4 depicts the disturbance invariant set \mathbb{Z}_k in Equation (9) and reachable set \mathbb{R}_k in Equation (16) along the trajectories for $\varepsilon = 0.01$ in the solution of robust tracking tasks. Additionally, Figure 3 compares the conservativeness of the reachability-based method with that of the tube MPC method by evaluating the areas of the reachable sets and disturbance sets generated by each approach. This figure presents the average area and standard deviation of the set areas for each trajectory at each step, represented by solid lines and ribbon regions, respectively. As shown, the reachability-based method results in a significantly smaller average area compared to the tube MPC method. Additionally, the narrower band of the reachability-based method reflects consistent stability and reduced conservativeness throughout the trajectory.

Figure 5 depicts trajectories from different methods under perturbation $\varepsilon = 0.1$. Our method outperforms tube MPC in tracking the reference trajectory, resulting in smaller state errors. Notably, our method is capable of effectively tracking the uniformly lifting pendulum, with the tracking process being stable and free of oscillations. In contrast, the tube MPC method exhibits continuous oscillations during the tracking process, with θ and $\dot{\theta}$ exhibiting sinusoidal variations. The reason may root in the conservativeness of disturbance invariant set. Our method provides tight reach-

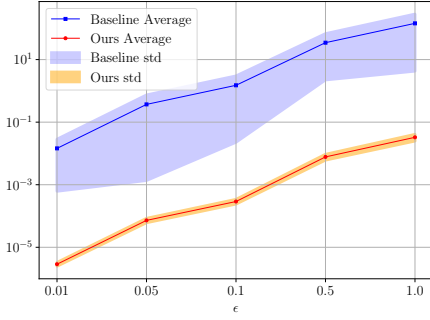


Fig. 3. Comparison of the average and variance of the set area between the tube MPC and reachability-based methods under varying levels of perturbation

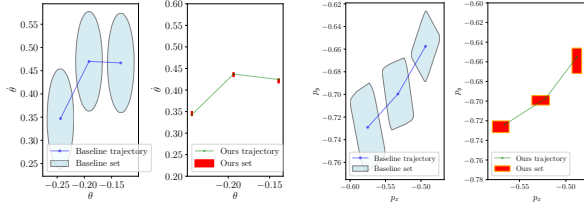


Fig. 4. Comparison of the disturbance invariant set and reachable set between the tube MPC method and the reachability-based method. Left: Pendulum, $\varepsilon = 0.01$; Right: DubinsCar, $\varepsilon = 0.1$.

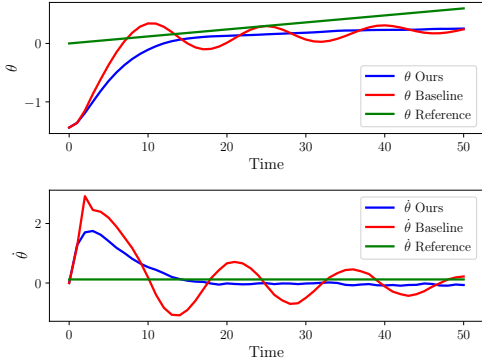


Fig. 5. Comparison of trajectories from different methods when $\varepsilon = 0.1$. Constant tracking error in state may due to short horizon of tracking problem and persistent disturbance on control input along the trajectory.

able set, which allows the optimization problem to compute more aggressive torque inputs to counteract the gravitational forces acting on the pendulum, resulting in a slow but stable trajectory tracking. On the other hand, the disturbance invariant set provided by tube MPC method is conservative, causing the solutions of optimization problem too insufficient to counteract gravity effectively. As a result, the pendulum repeatedly oscillates, failing to adequately track the reference state.

2) *DubinsCar*: First, we randomly sample an initial state from the set $\{[p_x, p_y, \alpha]^T \mid |p_x|, |p_y| \leq 1, \alpha = 0\}$ and apply control for 35 steps. Figure 6 illustrates the evolution of the reachable sets in the first two dimensions over time,

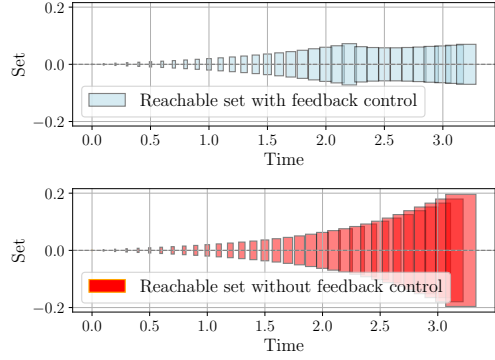


Fig. 6. Illustration of reachable sets with and without feedback over time for $\varepsilon = 0.01$. The center of each reachable set remains $y = 0$ at y -axis, with the x -axis representing the corresponding simulation time, where $dt = 0.1$. Although the state dimension of the DubinsCar model is three, this figure only shows the projection onto the first two dimensions for simplicity. The third dimension, representing the orientation angle, is naturally bounded within $[-\pi, \pi]$ and is omitted for clarity.

comparing scenarios with and without feedback control. With feedback control, the reachable set gradually expands, but remains bounded. In contrast, the reachable set of the system without feedback control grows exponentially.

Next, we randomly sample 20 initial and target states within $\{[p_x, p_y, \alpha]^T \mid |p_x|, |p_y| \leq 1, \alpha = 0\}$ and control 20 steps for each instance. The right plot of Figure 4 illustrates the disturbance invariant set \mathbb{Z}_k in Equation (9) and reachable set \mathbb{R}_k in Equation (16) for $\varepsilon = 0.1$ in the solution of robust tracking tasks. Observation shows that tube MPC method still offers a more conservative set than our method.

Figure 7 presents an example trajectory for different methods when $\varepsilon = 0.1$. In this figure, the trajectory generated by our method consistently follows the planned path, reaching the target position effectively. In contrast, the trajectory controlled by the tube MPC method first hovers near the initial position and then slowly approaching the target position. The behavior of tube MPC may be due to an overly conservative disturbance invariant set or inaccuracies in the

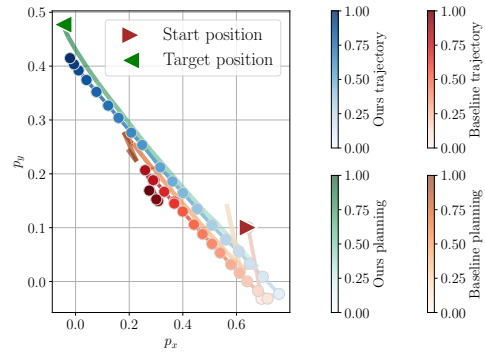


Fig. 7. Comparison of trajectories from different methods when $\varepsilon = 0.1$. Start position is (p_x^i, p_y^i) and Target position is (p_x^r, p_y^r) , which are the first two dimensions of \mathbf{x}_0 and \mathbf{x}_r . The color bar represents the car's movement over time, with darker shades indicating later time steps.

TABLE I

COMPARISON OF AVERAGE PER-STEP COST AND ERROR OF DIFFERENT METHOD UNDER VARIOUS PERTURBATION LEVEL UNDER PENDULUM AND DUBINS CAR ENVIRONMENTS

Pendulum	Ave per-step cost			Ave per-step err		
ε	1.0	0.1	0.01	1.0	0.1	0.01
Baseline	0.59	0.15	0.11	1.58	0.62	0.35
Reachability-based	0.18	0.13	0.11	0.58	0.38	0.34

DubinsCar	Ave per-step cost			Ave per-step err		
ε	1.0	0.01	0.001	0.1	0.01	0.001
Baseline	0.53	0.45	0.68	0.30	0.28	0.27
Reachability-based	0.32	0.41	0.64	0.23	0.21	0.25

TABLE II

COMPARISON OF COMPUTATION TIME FOR DISTURBANCE SET AND REACHABLE SET CALCULATIONS, ALONG WITH IPOPT SOLVING TIME, ACROSS DIFFERENT METHODS AND SCENARIOS WHEN $\varepsilon = 0.1$.

Time(s)		Set		IPOPT	
$\varepsilon = 0.1$		Baseline	Ours	Baseline	Ours
Pendulum	Average	0.009	0.004	0.222	0.018
	Std	0.004	0.002	0.144	0.014
DubinsCar	Average	0.744	0.007	4.830	2.762
	Std	0.051	0.002	3.548	2.688

system dynamics during linearization, leading to suboptimal control performance.

Additionally, we show our advantage in terms of control cost and tracking error. Table I presents a comparison of the average per-step control costs and average per-step control error, defined as $e_k = \|\mathbf{x}_k - \mathbf{r}_k\|_2$, across different methods under varying disturbance bounds of different environments. The results demonstrate that our method largely reduces the deviation between the actual and reference state and per-step control cost, which significantly outperforms the tube MPC method. Section IV-C.2 illustrates the computational advantage of our method in terms of reachable set and IPOPT optimization, compared to the disturbance invariant set computation and IPOPT solving in the tube MPC method. In this table, *Set* refers to the disturbance invariant set for the tube MPC method and the reachable set for our method. It's important to note that the computation times presented are for a 1-step look-ahead setting, and additional experiments are needed to assess performance in multi-step look-ahead scenarios.

Furthermore, we compare the reachability-based method with a naive approach that ignores disturbance when solving robust tracking problem but accounts for disturbances on control inputs. Tracking tasks are set near the constraint boundaries, with initial states sampled close to them. Trajectory is expected to closely follow the boundaries without violations as shown in Figure 2. Table III shows that the reachability-based method outperforms the naive one. The naive approach uses aggressive control, leading to constraint violations and higher costs, especially near boundaries as shown in Figure 8. In contrast, the reachability-based method successfully balances conservativeness and robustness.

TABLE III

COMPARISON OF AVERAGE PER-STEP COST AND ERROR OF DIFFERENT METHOD UNDER PERTURBATION $\varepsilon = 1.0, 0.1, 0.01$ WHEN INITIAL STATE AND TARGET STATE ARE NEAR THE CONSTRAINTS

DubinsCar	ave per-step cost			ave per-step err		
ε	1.0	0.1	0.01	1.0	0.1	0.01
Naive	1.027	0.397	0.347	0.097	0.056	0.050
Reachability-based	0.990	0.367	0.335	0.157	0.051	0.048

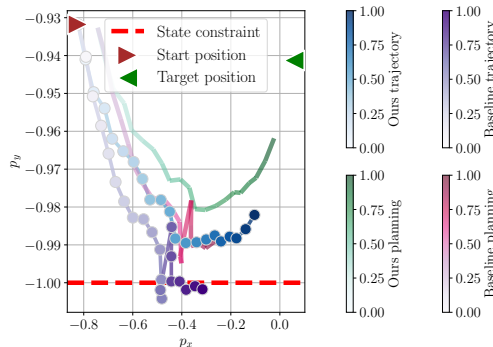


Fig. 8. Comparison of trajectories from different methods when $\varepsilon = 0.1$. The color bar represents the car's movement over time, with darker shades indicating later time steps.

V. CONCLUSION

This paper proposes a control method based on reachability analysis for the robust tracking problem with discrete-time neural network dynamic models (NNDM) and additive bounded perturbations on the control input. We first introduce a k -step reachability analysis tool specifically designed for NNDM, and then demonstrate how to incorporate the reachable set into the robust tracking control problem to ensure constraint satisfaction. Importantly, we prove the existence of a feedback control that bounds the growth of the reachable set and state error over an infinite horizon. Finally, simulation results show the efficacy of our method in terms of both conservativeness and control cost in comparison with typical tube MPC. Given that the IPOPT solver may produce suboptimal solutions for nonlinear optimization [23], future work will explore mixed-integer programming for exact solutions [5] or Bernstein polynomial approximations to accelerate solving process [4]. Further research may also focus on computing forward invariant sets to ensure persistent feasibility.

ACKNOWLEDGMENT

This work is in part supported by National Science Foundation under Grant No. 2144489. The authors would like to thank Xusheng Luo for his help in the revision of the paper.

REFERENCES

- [1] A. Nagabandi, G. Kahn, R. S. Fearing, and S. Levine, "Neural network dynamics for model-based deep reinforcement learning with model-free fine-tuning," in *2018 IEEE international conference on robotics and automation (ICRA)*, pp. 7559–7566, IEEE, 2018.

- [2] Z. Liu, G. Zhou, J. He, T. Marcucci, F.-F. Li, J. Wu, and Y. Li, "Model-based control with sparse neural dynamics," *Advances in Neural Information Processing Systems*, vol. 36, 2023.
- [3] D. Nguyen-Tuong and J. Peters, "Model learning for robot control: a survey," *Cognitive processing*, vol. 12, pp. 319–340, 2011.
- [4] H. Hu, J. Lan, and C. Liu, "Real-time safe control of neural network dynamic models with sound approximation," in *6th Annual Learning for Dynamics & Control Conference*, PMLR, 2024.
- [5] T. Wei and C. Liu, "Safe control with neural network dynamic models," in *Learning for Dynamics and Control Conference*, pp. 739–750, PMLR, 2022.
- [6] C. Liu and M. Tomizuka, "Control in a safe set: Addressing safety in human-robot interactions," in *Dynamic Systems and Control Conference*, vol. 46209, p. V003T42A003, American Society of Mechanical Engineers, 2014.
- [7] T. Wei and C. Liu, "Safe control algorithms using energy functions: A unified framework, benchmark, and new directions," in *2019 IEEE 58th Conference on Decision and Control (CDC)*, pp. 238–243, IEEE, 2019.
- [8] D. R. Agrawal and D. Panagou, "Safe control synthesis via input constrained control barrier functions," in *2021 60th IEEE Conference on Decision and Control (CDC)*, pp. 6113–6118, IEEE, 2021.
- [9] L. Chisci, J. Rossiter, and G. Zappa, "Systems with persistent disturbances: predictive control with restricted constraints," *Automatica*, vol. 37, no. 7, pp. 1019–1028, 2001.
- [10] W. Langson, I. Chrysochoos, S. Raković, and D. Mayne, "Robust model predictive control using tubes," *Automatica*, vol. 40, no. 1, pp. 125–133, 2004.
- [11] J. Lofberg, "Approximations of closed-loop minimax mpc," in *42nd IEEE International Conference on Decision and Control (IEEE Cat. No.03CH37475)*, vol. 2, pp. 1438–1442 Vol.2, 2003.
- [12] P. J. Goulart, E. C. Kerrigan, and J. M. Maciejowski, "Optimization over state feedback policies for robust control with constraints," *Automatica*, vol. 42, no. 4, pp. 523–533, 2006.
- [13] D. Bernardini and A. Bemporad, "Scenario-based model predictive control of stochastic constrained linear systems," in *Proceedings of the 48th IEEE Conference on Decision and Control (CDC) held jointly with 2009 28th Chinese Control Conference*, pp. 6333–6338, 2009.
- [14] D. de la Penad, A. Bemporad, and T. Alamo, "Stochastic programming applied to model predictive control," in *Proceedings of the 44th IEEE Conference on Decision and Control*, pp. 1361–1366, 2005.
- [15] J. Sieber, S. Bennani, and M. N. Zeilinger, "A system level approach to tube-based model predictive control," *IEEE Control Systems Letters*, vol. 6, p. 776–781, 2022.
- [16] B. Xue, M. Fränzle, and N. Zhan, "Under-approximating reach sets for polynomial continuous systems," in *Proceedings of the 21st International Conference on Hybrid Systems: Computation and Control (part of CPS Week)*, pp. 51–60, 2018.
- [17] B. Xue, M. Fränzle, and N. Zhan, "Inner-approximating reachable sets for polynomial systems with time-varying uncertainties," *IEEE Transactions on Automatic Control*, vol. 65, no. 4, pp. 1468–1483, 2019.
- [18] I. Kolmanovsky and E. G. Gilbert, "Theory and computation of disturbance invariant sets for discrete-time linear systems," *Mathematical problems in engineering*, vol. 4, no. 4, pp. 317–367, 1998.
- [19] H. Zhang, T.-W. Weng, P.-Y. Chen, C.-J. Hsieh, and L. Daniel, "Efficient neural network robustness certification with general activation functions," *Advances in neural information processing systems*, vol. 31, 2018.
- [20] C. Liu, T. Arnon, C. Lazarus, C. Strong, C. Barrett, M. J. Kochenderfer, et al., "Algorithms for verifying deep neural networks," *Foundations and Trends® in Optimization*, vol. 4, no. 3-4, pp. 244–404, 2021.
- [21] L. Chisci, J. Rossiter, and G. Zappa, "Systems with persistent disturbances: predictive control with restricted constraints," *Automatica*, vol. 37, no. 7, pp. 1019–1028, 2001.
- [22] A. Wächter and L. T. Biegler, "On the implementation of an interior-point filter line-search algorithm for large-scale nonlinear programming," *Mathematical programming*, vol. 106, pp. 25–57, 2006.
- [23] M. Housh, "Optimization of multi-quality water networks: Can simple optimization heuristics compete with nonlinear solvers?," *Water*, vol. 13, no. 16, p. 2209, 2021.